

LIGHTWEIGHT BUMPERS EMPLOYING MULTIPLE MESHES

Friedrich Hörz*, Mark J. Cintala*, Ronald P. Bernhard** and Thomas H. See**

*NASA Johnson Space Center, Houston, TX 77058, USA

**Lockheed-ESC, 2400 NASA Rd. 1, Houston, TX 77058, USA

ABSTRACT

Through controlled laboratory experiments we demonstrate that laterally discontinuous targets, such as meshes, will comminute hypervelocity projectiles with efficiencies comparable to that of continuous, sheet-like materials of identical thickness (and material). Substantial mass savings in current collisional bumper designs seem possible if continuous bumper components were replaced by meshes. A series of successive mesh layers seems particularly attractive because multiple collisions -- as described by others and substantiated by the present experiments -- promotes melting, comminution, dispersion, and deceleration of impactor fragments, compared to monolithic targets of identical, specific areal mass (g/cm^2).

1. INTRODUCTION

Shock theory does not require that a collisional bumper be laterally continuous. Shock waves sufficient to vaporize, melt, comminute, disperse, and decelerate hypervelocity impactors are readily produced by targets that have dimensional scales comparable to, if not much smaller than, typical projectile diameters (D_p). For example, at impact velocities of 6 km/s, fragmentation of glass projectiles is induced by very thin aluminum foils of thickness (T) equal to $0.003 D_p$ (Ref. 1). In addition, we routinely expose thin, electrically biased tungsten wires in our light-gas gun to investigate/collect impact generated plasma; glass and aluminum impactors of a few millimeter in diameter are completely shattered if they collide (inadvertently) with these wires ($T=0.02 D_p$). Thus, relatively thin wires or delicate meshes should be suitable as collisional bumper components. Compared to solid sheets that are typically employed in ongoing bumper developments (e.g., Refs. 2-7), such "discontinuous" mesh materials may offer substantial mass savings.

A highly idealized, discontinuous bumper composed of multiple-mesh layers is conceptualized in Figure 1. Successive mesh layers produce repetitive shocks in the projectile and its fragments, and constitute a particularly effective means to promote heating, comminution, dispersion, and deceleration of hypervelocity impactors (e.g., Refs. 8, 9, 10). Each mesh is constructed from wires of either square or round cross-section, such that dimension T may define both the vertical and lateral extent of a single wire target. Each successive mesh in Figure 1 is a half-scale version of the preceding mesh with regard to wire thickness (T) and mesh size (M). The first, most massive mesh has dimensions that are totally dictated by the largest projectile (of diameter D_p) against which protection is being sought by the entire bumper stack. Center-to-center distance (M) of individual wires equals D_p , thereby assuring that mesh opening (M_o) is $M_o = (D_p - T)$, and that physical contact between the projectile and mesh wires is being made. Wire thickness T relative to D_p is presently undefined and must be constrained by dedicated

experimental and theoretical inquiries. Operationally, however, T must be such that the (first) mesh disrupts the impactor into fragments $< 1/2 D_p$ in size, regardless of where the impactor hits on the mesh target. Materials reaching the second mesh will be subjected to additional comminution and all fragments that exit the second mesh should have sizes $< 0.25 D_p$. Any number of correspondingly scaled mesh layers may be stacked to provide successive comminution opportunities. The n^{th} mesh, of dimensions T_n and M_n , will control the smallest fragment size (F_n) that is permitted to exit the entire stack ($F_n < M_n$). Absolute dimensions M and T of the first mesh are crucial for the cumulative, specific areal mass (SM ; g/cm^2) of the entire bumper stack, because all additional meshes are merely dimensionally scaled versions of M and T for this first mesh.

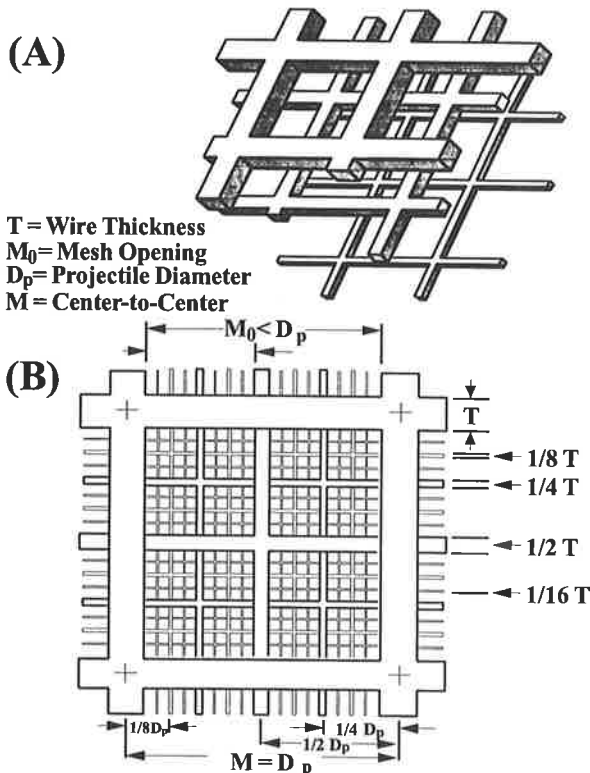


Figure 1. Discontinuous bumper concept that employs multiple mesh layers which are dimensionally scaled to the diameter of the projectile (D_p) that can be terminated by the entire stack (see Ref. 11).

This contribution summarizes the utility of aluminum wire meshes as potential bumper components by synthesizing three major reports that addressed the fragmentation behavior of glass projectiles upon encounter with (1) continuous aluminum targets of $T=0.0005$ to $5 D_p$ (Ref. 1), (2) a single aluminum mesh to explore the effects of T and to establish a possible minimum value for T (Ref. 11), and (3) multiple-mesh

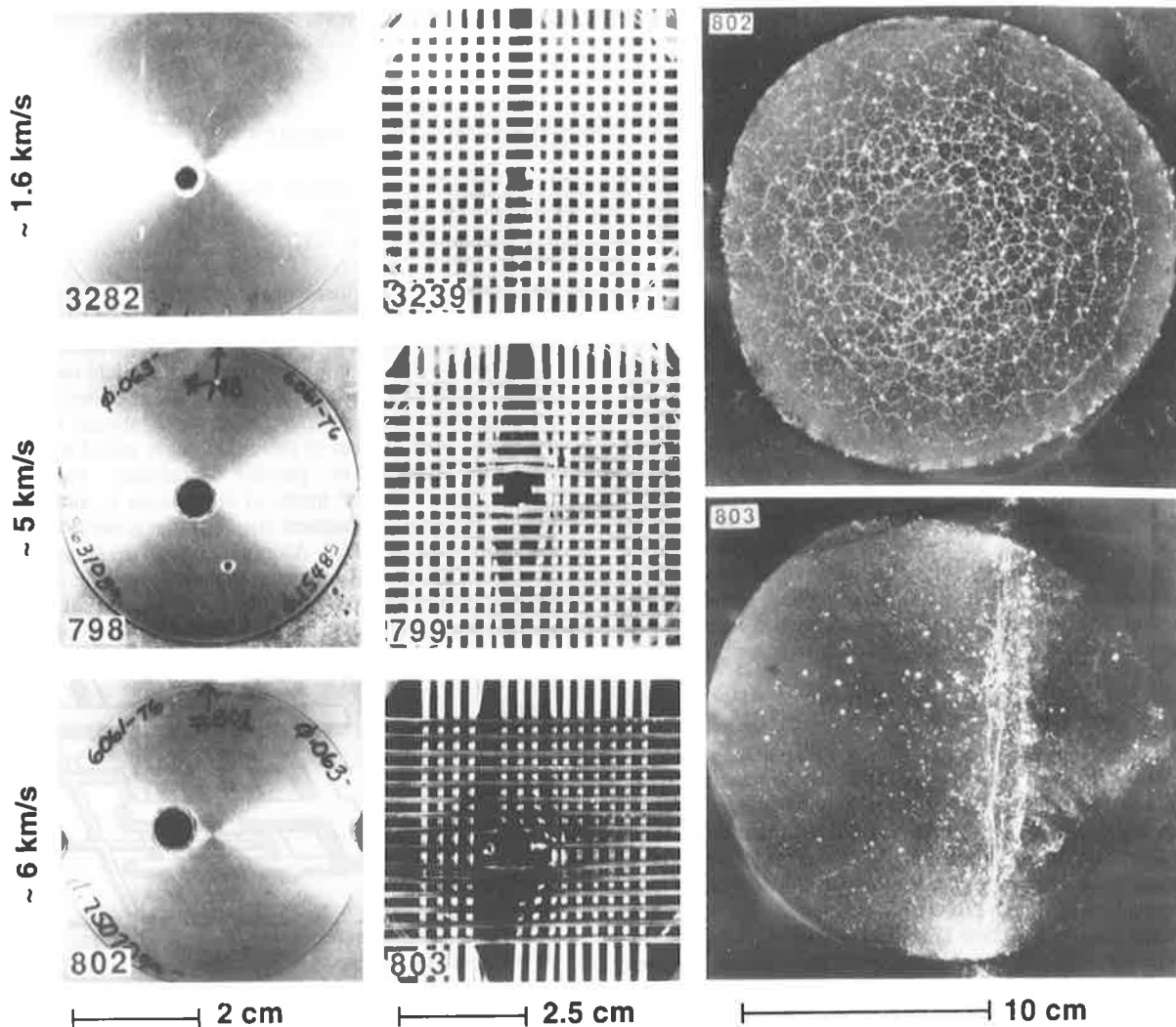


Figure 2. Damage sustained by continuous (left) and discontinuous (center) targets of $T=0.5 D_p$ that were struck by glass impactors at velocities of 1.6, 5 and 6 km/s. The witness plates for experiments 802 and 803 (right) are shown to illustrate the differences in the mass distribution of debris clouds emanating from continuous (top) and discontinuous (bottom) targets.

bumpers composed of custom-manufactured or commercial-aluminum meshes (Ref. 12). For detailed experimental procedures, methods of analysis, extensive photo-documentation and additional results the reader is referred to these original, detailed reports.

The extensive background studies on continuous targets (Ref. 1) employed soda-lime glass projectiles because they supported the development of cosmic-dust flight instruments; in comparison, the dedicated mesh experiments were modest efforts and silicate impactors were retained for reasons of internal consistency. Clearly, there is no single projectile material that adequately simulates the pertinent physical properties of all particle types in low-Earth orbit (LEO). As revealed by recent Long Duration Exposure Facility (LDEF) investigations (Ref. 13), natural silicates are, at present, the most abundant particle type in LEO at $D_p < 1$ mm; the need for duplicate experiments with metal impactors, however, is unquestioned.

2. EXPERIMENTAL RESULTS

2.1 Comparison of Single-Foil and Single-Mesh Targets

Figure 2 illustrates the degree of damage typically suffered by continuous membranes (left) and discontinuous meshes (center). Figure 3 shows the relationship between target thickness (T) and the diameter of the resulting penetration hole

(D_h) in continuous targets of varying T that were penetrated by projectiles ranging from 50 to 3175 μm in diameter. The purpose is to show that linear scaling of the projectile size is a useful, first-order approach to predict the amount of damage sustained by targets of $T < D_p$ (at constant impact velocity of ~ 6 km/s). Penetrations of massive, contiguous targets are viewed as truncated cratering events, having hole diameters some 4 to 5 times larger than D_p ; the condition of $D_h = D_p$ is approached at $T < 0.01 D_p$. The penetration holes in the mesh targets exhibit similar trends: the length of wire cut and physically removed from the mesh corresponds to D_h of the continuous targets, although the actual extent of mesh deformation is controlled (and enlarged) by plastic deformation and bending of the (non-dislodged) wire ends.

The total displaced mass was characterized for each penetration, either by weight difference of the target before and after an experiment, or by physical capture and collection of displaced debris (see Ref. 11, Figures 24-28). The total amount of mass displaced for the continuous targets is invariably higher than for single mesh targets, but it systematically relates to T for both cases. Specifically, the mass liberated during penetration of the targets relates to the specific mass (g/cm^2) of the bumper itself. Furthermore, the mass dislodged from the bumper can readily exceed that of the incoming projectile (e.g., Ref. 14, 15).

These results suggests that lightweight bumpers, in general, are to be preferred over more massive bumpers. Lightweight

bumper designs -- at otherwise equivalent performance -- produce fewer particulates that may potentially damage an underlying flight system or which may be added to the existing population of space debris. These observations constitute strong technical arguments to deploy the most lightweight bumpers possible for any desired degree of protection. Traditionally, the major motivation to produce lightweight bumpers relates to programmatic concerns, such as increased launch mass, effective payload penalties, and associated costs. We stress that programmatic, as well as *technical* arguments combine to call for the most lightweight bumpers possible.

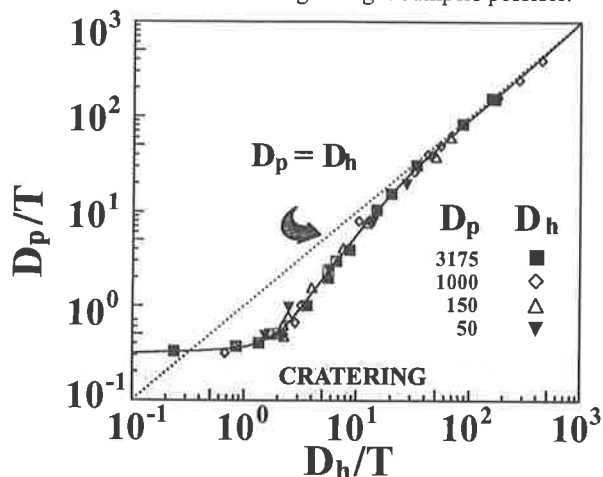


Figure 3. The relationship of projectile diameter (D_p ; μm), target thickness (T), and penetration-hole diameter (D_h) for continuous aluminum targets that were impacted by soda-lime glass spheres traveling at 6 km/s.

Each of our experiments employed a witness plate of aluminum (series 1100, annealed; 30 x 30 cm in size, 1.6 or 3.2 mm thick, and 10 to 12 cm behind the last mesh layer) to monitor the debris cloud emanating from the test article. Examples of two such witness plates are shown in Figure 2 (right). The debris clouds which encounter these witness plates are a mixture of projectile fragments and dislodged bumper material (e.g., Refs. 14, 15, 16). While the damage patterns associated with such debris clouds are geometrically complex, they systematically depend on T for both continuous (e.g., Refs. 1, 14) and single-mesh targets (Ref. 11). Note the symmetric debris pattern of the continuous target, and a pronounced linear damage patterns for the single-mesh example (Figure 2). The resulting debris clouds reflect the mass distribution of the targets and substantiate the above notion that the mass displaced from the bumper can totally dominate the damage inflicted to a flight system.

The distinctly linear, highly localized streaks resulting from the mesh penetration(s) are undesirable for collisional bumper purposes. They represent localized maxima in energy deposition that contain specific energies (erg/cm^2) in excess of those characterizing the more homogenized and substantially centro-symmetric debris clouds from continuous targets.

Generally, all witness plates do not possess a single, outstandingly large crater, but a number of craters instead, all of comparable size. The size of these "largest" craters, however, strongly depends on T for both continuous and discontinuous targets. The absolute number of craters is generally higher for continuous targets than for mesh targets. These observations suggests that T systematically controls the size of the largest fragment(s) and that the total specific bumper mass affects the frequency of these craters. Our thinnest wires had relative dimensions of $T=0.08 D_p$; these wires shattered both glass and aluminum projectiles into numerous pieces, all substantially smaller than $0.5 D_p$. The thinnest foils tested had $T=0.0003 D_p$, which did not disrupt the projectile. Based on extensive tests with thin foils, the condition where the largest fragment remaining may approach

$0.5 D_p$ in size is estimated to occur at $T=0.001-0.005 D_p$ (see Ref. 1). Therefore, relatively thin wires, and meshes of much higher transparency than are illustrated in Figure 1 may readily suffice as efficient bumpers.

In summarizing the above comparisons of single foil and mesh penetrations, we conclude that the target thickness is the parameter of overwhelming significance. It controls the diameter of the displaced target area and, therefore, the total displaced bumper mass. More importantly, it also controls the degree of projectile comminution (Ref. 1); collisions with wires and foils of constant T yield comparable fragmentation products. These observations substantiate our basic premise that targets do not need to be laterally continuous to accomplish substantial disruption of hypervelocity impactors. We also learned that relatively thin targets will produce substantially disrupted projectiles, a conclusion that permits and encourages the use of highly transparent and relatively lightweight meshes as bumper components.

Table 1. Pertinent experimental conditions for select experiments illustrated in this report. All projectiles were 3.175 mm in diameter.

Exp. No.	Vel. km/s	M mm	T mm	N	S mm	SM g/cm^2
798	5.00	cont.	1.6	1	NA	0.424
799	5.20	3.17	1.6	1	NA	0.333
802	6.02	cont.	1.6	1	NA	0.424
803	5.91	3.17	1.6	1	NA	0.333
813	5.76	3.17	0.305	1	NA	0.016
822	6.07	3.17	0.305	2	NA	0.032
823	5.77	3.17	0.305	3	25.4	0.048
975	5.89	3.17	0.305	5	25.4	0.080
979	5.86	3.17	0.305	10	25.4	0.160
982	5.74	1.59	0.254	10	25.4	0.180
989	5.81	1.59	0.254	10	12.7	0.180
990	5.97	1.59	0.254	10	50.8	0.180
991*	5.90	1.59	0.254	10	50.8	0.180
3422	1.02	1.59	0.254	10	50.8	0.180
3423	1.95	1.59	0.254	10	50.8	0.180

*aluminum projectile; all others soda-lime glass

2.2 Multiple-Mesh Stacks

The tests employing multiple-mesh layers proceeded along a parametric matrix that included velocity (1-6 km/s), the number of meshes (N ; 1-10), separation distance between mesh layers (S ; 12-100 mm), mesh-size (M ; 1.6 and 3.2 mm), and the total bumper mass (SM ; 0.01-1.0 g/cm^2) as the variables of major interest. Figures 4 and 5 display typical experimental products, while Table 1 details pertinent, initial conditions for the illustrated tests (see Ref. 12 for additional details). All tests were performed with 3.175 mm diameter projectiles. The specific areal mass of the glass impactor was 0.467 g/cm^2 ; note from Table 1 that most multiple-mesh tests contained less than half the mass of the projectile.

Figure 4 illustrates the damage suffered by each of ten identical mesh layers that composed experiment 991, one of the few tests employing an aluminum projectile. As can be seen in Figure 4, the central portion of the expanding debris cloud forcefully plowed through mesh 5, to be rather abruptly terminated by mesh 6. However, a few, small fragments continued through mesh 10, owing to the intrinsic transparency of mesh stacks. Silicate impactors exhibit grossly similar behavior (at 6 km/s) to the aluminum projectile in Figure 4, yet dispersion of glass projectiles is noticeably less, resulting in modestly deeper penetrations for dense silicate impactors, typically to meshes 7-9, and smaller diameters of penetration holes throughout the stack.

Diameter measurements of the penetration holes in the various mesh layers (Ref. 12) reveal that they do not correspond to a geometrically linear dispersion of the debris cloud through the successive layers. Instead, these holes exhibit distinctly

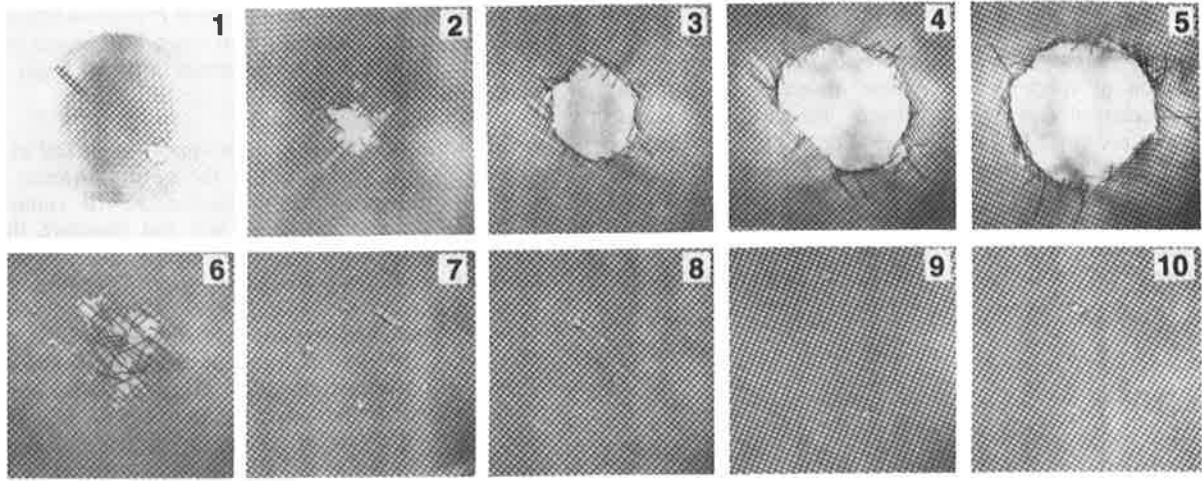


Figure 4. Damage in successive mesh layers caused by a 3.175 mm diameter aluminum impactor ($D_p=3.175$ mm) traveling at ~ 5.9 km/s. Separation distance (S)= $16 D_p$, $M=0.5 D_p$, $T=0.08 D_p$, and $SM=0.18$ g/cm².

successive layers. Instead, these holes exhibit distinctly stepped diameters, indicating that discrete, radial increments of the cloud's outer edge are being terminated. This stepped behavior not only applies until the maximum hole diameter is reached, but especially to the meshes immediately succeeding this mesh, where most of the debris is being terminated over a relatively short distance by a small number of meshes. Note in Figure 4 that a single mesh (*i.e.*, mesh 6) suffices to terminate most debris that exits mesh 5.

Compared to glass impactors, aluminum impactors are decelerated/destroyed with greater efficiency at 6 km/s. Substantial melt (or vapor) deposits on the witness plates attest to entropy gains during multiple shock (*e.g.*, Ref. 9), sufficient to melt (or vaporize) aluminum in these specific experiments at ~ 6 km/s. This could be the reason for the unusually abrupt termination of particulate debris between meshes 5 and 6 in Figure 4. The glass projectiles, on the other hand, did not produce equivalent melt or vapor-deposits on the witness plates; most fragments must have remained unmolten, the reason why they penetrated deeper into the mesh-stack. However, at lower velocities (~ 2 km/s) the reverse is true. The aluminum impactors remain essentially intact, due to their high tensile strength, and they readily penetrated an entire stack of 10 meshes, while the glass impactors were thoroughly comminuted, dispersed and decelerated.

Figure 5 presents typical witness plates in order to visualize the general characteristics of the debris cloud in response to some of the major variables investigated. The top two rows illustrate experiments that employed 1, 2, 3, 5 and 10 identical mesh layers; test 982 employed a finer mesh than 979 at otherwise identical conditions (see Table 1). Note that the addition of each single mesh layer not only adds to the degree of comminution (resulting in smaller and more numerous witness plate craters), but also to an increasingly more homogeneous mass and energy distribution of the debris cloud. Some 2 to 3 meshes suffice to yield spatial distributions of fragment sizes and energies akin to those of solid sheets of equivalent, cumulative mass; five or more mesh layers invariably outperformed a single sheet, as evidenced by the smaller diameter of the damage patterns that are caused by increasingly finer-grained debris. Finer mesh-sizes are, undoubtedly, highly beneficial (*e.g.*, 979 versus 982 in Figure 5), as they offer an increased number of interactions between the target and the projectile, resulting in a finer-grained debris, less of which reaches the witness plate.

Among the variables tested, the separation distance (S) between individual mesh layers was found to play a major role, as noted by others (*e.g.*, Ref. 9, 10) for multiple-foil targets. Experiments 989, 982 and 990 (Figure 5, middle row)

utilized separation distances of 12.5, 25 and 50 mm, respectively. Increased S permits better dispersion of the debris cloud between successive mesh layers, such that overlapping penetration events, especially by the large, central fragments, occur with decreased frequency, if at all. Note that witness plate 990 has no discrete secondary craters, but only a pronounced thermal aureole. Clearly, the larger the separation distance, the better.

The effects of velocity are comparatively modest, at least for silicate impactors (*e.g.*, 3422, 3423 and 990 in Figure 5). There is little doubt that low-velocity (<2 km/s) glass impactors disperse and fragment less efficiently than those traveling at >4 km/s, as evidenced by the smaller penetration holes in all mesh layers. However, the debris cloud is less energetic at the low velocities and is, therefore, largely terminated by ten-mesh bumpers. This relative insensitivity to encounter velocities seems to be a highly favorable property of mesh bumpers, but more tests with metal impactors are needed to better isolate the basic effects of multiple-mesh interactions from those related to projectile rheology.

All of the above tests were conducted with identical mesh layers per experiment. Systematically scaled meshes, as illustrated in Figure 1, were only utilized in a few experiments. The most delicate mesh available was the commercial screen ($T=0.08 D_p$) used in experiment 991 (Figure 4). The more massive members of these scaled mesh stacks had to employ relatively thick wires, which rapidly resulted in very unfavorable mass properties ($SM>0.5$ g/cm²). Furthermore, thick wires produced excessively massive debris clouds and large individual fragments that frequently could not be terminated by the relatively delicate mesh layers towards the rear of the stack. The so called "mixed" stacks tested during this study were simply too massive and their performance was vastly inferior to bumper arrangements described in Table 1. However, this does not invalidate the concept suggested in Figure 1. It was merely not possible, within the scope of this effort, to acquire suitably dimensioned meshes to perform more rigorous tests of dimensionally scaled, multiple-mesh bumpers.

2.3 Comparison With Other Lightweight Bumpers

To initiate comparisons with more fully developed bumper and shield designs (*e.g.*, Ref. 10), we performed a few experiments that employed a contiguous *rear wall* (0.5 mm thick; aluminum 2024). The purpose of this rear wall is to produce a totally opaque shield that keeps even the most fine-grained debris from reaching a flight system. Obviously, this is the ideal extreme for collisional shields, but we note that a fair number of flight systems will be able to tolerate some fine-

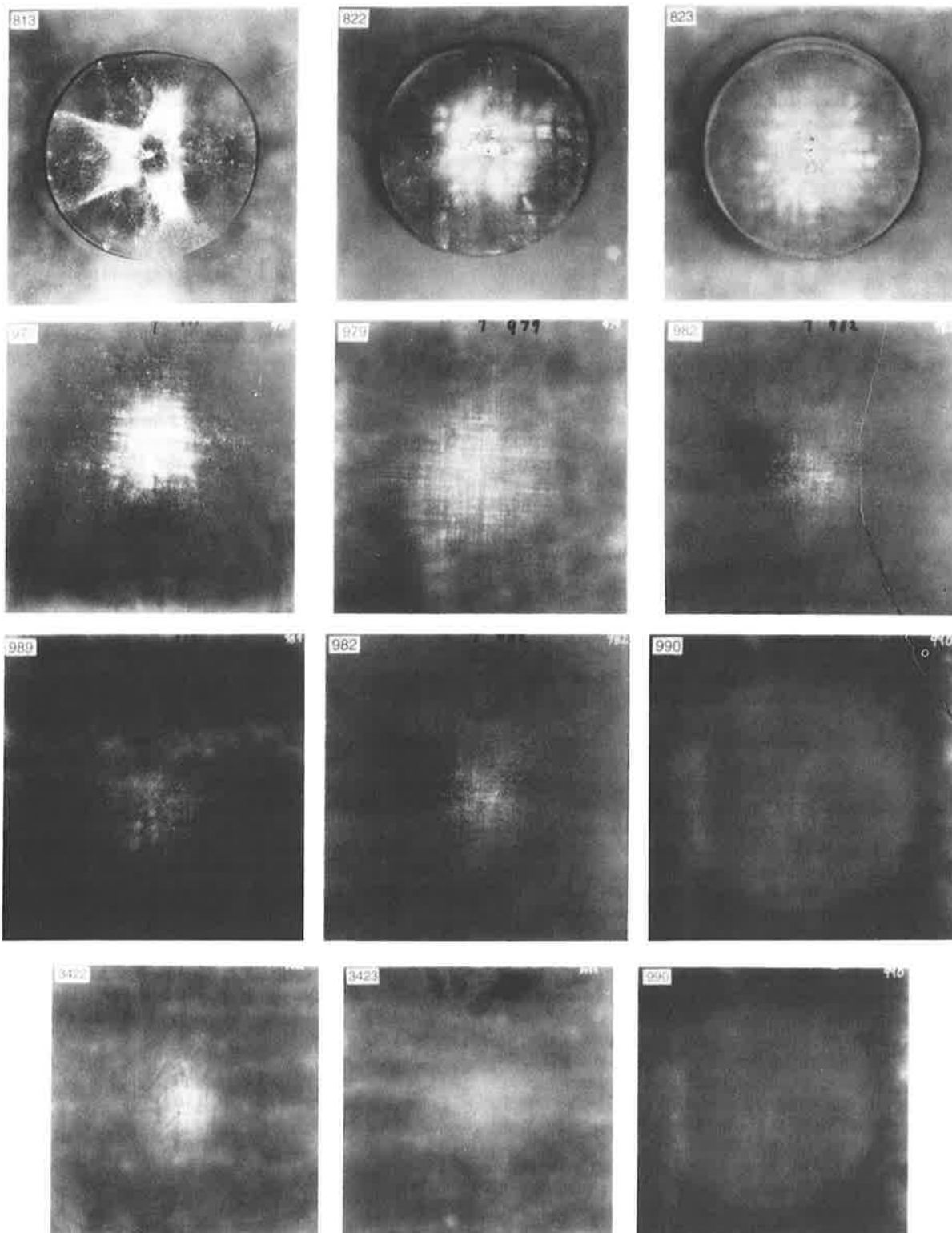


Figure 5. Representative witness plates (30 x 30 cm) of multiple-mesh bumper tests. Experiment number is in upper left hand corner for cross reference with Table , which details experimental conditions. Experiments 813 through 979 (left to right) employed 1, 2, 3, 5 and 10 mesh layers, respectively, all at projectile velocities of ~6 km/s. Experiment 982 and 979 illustrate the effects of mesh size. Experiments 989, 982 and 990 illuminate the effects of separation distance (S). The bottom row illustrates the effects of velocity with 3422, 3423, and 990 at ~1.02, 1.95 and 5.97 km/s, respectively.

grained, low-velocity debris and will not require totally opaque shielding. Leading concepts among totally opaque shields are the so called "Multi-Shock" (MS) design (Ref. 9) and the "Mesh-Double-Bumper" (MDB) concept (Refs. 10, 17). Note that the MDB design independently advocates the use of a single mesh on the bumper entrance side. The most recent, optimized MS and MDB concepts (Ref. 6) typically possess

specific areal masses of 0.3 g/cm^2 , at experimental conditions equivalent to ours. However both designs utilize a total shield depth (ΣS ; sum of all separation distances) of ~10 cm, whereas our stacks employed depths which were typically two to five times larger (see Table 1). This is a significant difference considering how much the separation distance affects the overall bumper performance (see Figure 5).

The current feasibility study and associated hardware did not permit exact analog studies with such optimized MS and MDB shield designs. Nevertheless, we compressed our ten-member stacks to 14 cm total depth, including the rear wall. This arrangement possessed a cumulative SM of 0.314 g/cm^2 , and turned out to be ideally opaque to a $\sim 3.2 \text{ mm}$ diameter aluminum projectile traveling at $\sim 5.8 \text{ km/s}$. Removal of one mesh, to decrease ΣS , resulted in two small penetrations of the rear wall. Another totally opaque shield used 16 mesh layers ($T=0.08 D_p$) and a relatively thin rear wall, resulting in $SM=0.34 \text{ g/cm}^2$ over a distance (ΣS) of 11 cm. These few experiments demonstrate that the performance of aluminum, multiple-mesh bumpers is comparable to the current MS and MDB designs.

Note that the MS and MDB designs derive substantial benefits from the utilization of state-of-the-art, lightweight materials possessing favorable dynamic properties (e.g., NEXTEL, a ceramic fiber cloth; KEVLAR; etc.; see Ref. 9). Furthermore, these materials are typically stranded from multiple, ultra-fine twines, which produce much more finer-grained debris than monolithic targets. If meshes of suitable dimensions could be manufactured from materials with such favorable properties, additional and significant mass savings seem possible relative to all current shield concepts.

3. SUMMARY

We have demonstrated that continuous membranes and discontinuous mesh targets, made from aluminum, result in comparable degrees of projectile disruption for any given target thickness. Comparatively thin targets ($T < 0.1 D_p$) suffice to cause substantial collisional fragmentation of glass and aluminum impactors at $\sim 6 \text{ km/s}$. Relatively massive targets, of $T > 0.5 D_p$, seem undesirable because they result in excessively massive and energetic debris clouds. Multiple component bumpers that precipitate repetitive shocks can be constructed from very thin, lightweight materials. Bumper performance will improve with an increasing number of individual layers and increasing separation distance; the largest practical separation distance should be sought for any flight design, because it translates directly into bumper mass needed to defeat a hypervelocity impactor. These conclusions apply to all bumpers, whether continuous or discontinuous.

Nevertheless, the intrinsic transparency of meshes affords potentially significant weight savings over continuous bumper components in most (all) circumstances. It simply is not necessary to expose laterally continuous targets. Relatively thin wires/solids suffice to disrupt, disperse and decelerate hypervelocity impactors. Indeed, each mesh could be replaced by only rows of thin wires, all at spacing $< D_p$; such parallel wire-systems would be all that is needed from a shock point of view. Thus, half of the *current* mesh mass would fundamentally suffice to do an adequate job of disrupting, dispersing and decelerating any impactor. There seems little doubt that discontinuous bumper materials should be given serious consideration in future bumper developments, even more so if lightweight, stranded solids of favorable dynamic properties were manufactured into suitably dimensioned meshes or other regular geometries of $M_o < D_p$.

4. REFERENCES

- Hörz, F., Cintala, M.J., Bernhard, R.P., and See, T.H., Dimensionally Scaled Penetration Experiments: Aluminum Targets and Glass Projectiles $50 \mu\text{m}$ to 3.2 mm in Diameter, submitted to *Int. J. Impact Engn.*, 1993.
- Whipple, F.L., The Meteoritic Risk to Space Vehicles, *Proc. Intl. Astronomical Congress*, Springer Verlag, Wien, 418-428, 1958.
- Kinslow, R., ed., *High-Velocity Impact Phenomena*, Academic Press, New York, 579 p., 1970
- Anderson, C.E, ed., Hypervelocity Impact, Proceedings of the 1986 Symposium, *Int. J. Impact Engn. Vol. 5*, 759 p, 1987.
- Anderson, C.E., ed., Hypervelocity Impact, Proceedings of the 1989 Symposium, *Int. J. Impact Engn., Vol. 10*, 639 p., 1990.
- Anderson, C.E., ed., Hypervelocity Impact, Proceedings of the 1992 Symposium, *Int. J. Impact Engn.*, in press.
- Christiansen, E.L., Design and Performance Equations for Advanced Orbital Debris Shields, in *Hypervelocity Impact, Proc. 1992 Symposium*, Anderson, C.E., ed.; *Int. J. Impact Engn.*, submitted.
- Richardson, A.J., Theoretical Penetration Mechanics of Multi-Sheet Structures Based on Discrete Particle Modeling, *J. Spacecraft & Rockets, Vol. 7*, 486-489, 1970.
- Cour-Palais, B.G. and Crews, J.L., A Multi-Shock Concept for Spacecraft Shielding, *Int. J. Impact Engn., Vol. 10*, 135-146, 1990.
- Christiansen, E.L. and Kerr, J.K., Mesh Double-Bumper Shield: A Low Weight Alternative for Spacecraft Meteoroid and Orbital Debris Protection, in *Hypervelocity Impact, Proc. 1992 Symposium*, Anderson, C.E. ed., *Int. J. Impact Engn.*, submitted.
- Hörz, F., Cintala, M.J., See T.H., Bernhard, R.P., Cardenas, F., Davidson, W., and Haynes, J., Comparisons of Continuous and Discontinuous Bumpers: Dimensionally Scaled Impact Experiments into Single Wire Meshes, *NASA TM 104749*, 83 p, 1992.
- Hörz, F., Cintala, M.J., Bernhard, R.P., Cardenas, F., Davidson, W., Haynes, G., Winkler, J., and Gray, B., Impact Experiments into Multiple-Mesh Targets: Concept Development of a Light-Weight Collisional Bumper, *NASA TM 104764*, 1993.
- Bernhard, R.P., See, T.H., and Hörz, F., Composition and Modal Frequencies of Hypervelocity Particles $< 1 \text{ mm}$ in Diameter in Low-Earth Orbit, *Lunar Planet. Sci. XXIV*, in press.
- Pietkutowski, A.J., A Simple Dynamic Model for the Formation of Debris Clouds, *J. Int. Impact Engn., Vol. 10*, 453-471, 1990.
- Stilp, A.J., Hohler, V., Schneider, E., and Weber, K., Debris Cloud Expansion Studies, *Int. J. Impact Engn. Vol. 10*, 543-554, 1990.
- Schonberg, W.P., and Taylor, R.A., Penetration and Ricochet Phenomena in Oblique Hypervelocity Impacts, *AIAA Journal, Vol. 27*, 639-646, 1989.
- Christiansen, E.L., Advanced Meteoroid and Debris Shielding Concepts, *AIAA/NASA/DOD Orbital Debris Conference, AIAA 90-1336*, 14.p, 1990.